

4

RADC-TR-89-181
Final Technical Report
October 1989



HIGH SPEED SIGNAL EXTRACTION USING ELECTRO-OPTIC TECHNIQUES

University of Rochester

John Nees and Gerard Mourou

DTIC
ELECTE
NOV 16 1989
S B D

AD-A214 446

APPROVED FOR PUBLIC RELEASE; DISTRIBUTION UNLIMITED.

ROME AIR DEVELOPMENT CENTER
Air Force Systems Command
Griffiss Air Force Base, NY 13441-5700

86 11 10 012

UNCLASSIFIED
SECURITY CLASSIFICATION OF THIS PAGE

REPORT DOCUMENTATION PAGE				Form Approved OMB No. 0704-0188	
1a REPORT SECURITY CLASSIFICATION UNCLASSIFIED			1b RESTRICTIVE MARKINGS N/A		
2a SECURITY CLASSIFICATION AUTHORITY N/A			3 DISTRIBUTION AVAILABILITY OF REPORT Approved for public release; distribution unlimited.		
2b DECLASSIFICATION/DOWNGRADING SCHEDULE N/A					
4 PERFORMING ORGANIZATION REPORT NUMBER(S) N/A			5 MONITORING ORGANIZATION REPORT NUMBER(S) RADC-TR-89-181		
6a NAME OF PERFORMING ORGANIZATION University of Rochester		6b OFFICE SYMBOL (If applicable)		7a NAME OF MONITORING ORGANIZATION Rome Air Development Center (RBRP)	
6c ADDRESS (City, State, and ZIP Code) 250 East River Road Rochester NY 14623-1299			7b ADDRESS (City, State, and ZIP Code) Griffiss AFB NY 13441-5700		
8a NAME OF FUNDING SPONSORING ORGANIZATION Rome Air Development Center		8b OFFICE SYMBOL (If applicable) RBRP		9 PROCUREMENT INSTRUMENT IDENTIFICATION NUMBER F30602-81-C-0206	
8c ADDRESS (City, State, and ZIP Code) Griffiss AFB NY 13441-5700			10 SOURCE OF FUNDING NUMBERS		
			PROGRAM ELEMENT NO 62702F	PROJECT NO 2338	TASK NO 01
			WORK UNIT ACCESSION NO PM		
11 TITLE (Include Security Classification) HIGH SPEED SIGNAL EXTRACTION USING ELECTRO-OPTIC TECHNIQUES					
12 PERSONAL AUTHOR(S) John Nees and Gerard Mourou					
13a TYPE OF REPORT Final		13b TIME COVERED FROM Jan 86 to Sep 87		14 DATE OF REPORT (Year, Month, Day) October 1989	
15 PAGE COUNT 28					
16 SUPPLEMENTARY NOTATION N/A					
17 COSATI CODES			18 SUBJECT TERMS (Continue on reverse if necessary and identify by block number)		
FIELD	GROUP	SUB-GROUP	Optics		
14	04		Signal Extraction		
09	03				
19 ABSTRACT (Continue on reverse if necessary and identify by block number) The University of Rochester has done preliminary experiments on several test methods to determine which one could best provide a low loading test environment. The range of techniques considered for signal extraction included direct and external modulation of semiconductor laser light. For the laser based modulation both gain and loss control were considered. Under gain controlled laser modulation using available semiconductor lasers, the max. efficiency of the laser would cause unwanted current loading of the device under test (DUT). Using loss modulation in laser diodes, efficient modulation can be obtained with only small loading effects; however, these diodes are very temperature sensitive and will not give the necessary performance under a variety of temperatures. External modulation by electro-absorption was also inadequate due to temperature sensitivity. There are polymers which exhibit electro-optic co-efficients orders of magnitude greater than conventional crystals, but for some reason these effects fade with time. Finally, U of R considered confined wave modulators. The integrated Mach-Zender modulation can be directly connected to optical					
20 DISTRIBUTION AVAILABILITY OF ABSTRACT <input checked="" type="checkbox"/> UNCLASSIFIED/UNLIMITED <input type="checkbox"/> SAME AS RPT <input type="checkbox"/> DTIC USERS			21 ABSTRACT SECURITY CLASSIFICATION UNCLASSIFIED		
22a NAME OF RESPONSIBLE INDIVIDUAL Frederick G. Hall			22b TELEPHONE (Include Area Code) (315) 330-2241		22c OFFICE SYMBOL RADC (RBRP)

UNCLASSIFIED

Block 19 (Cont'd)

fibers without polarizers. This technique was the one determined to be the most viable in producing a low loading signal extraction method.

Accession For	
NTIS GRACI	<input checked="checked" type="checkbox"/>
DDIC TAB	<input type="checkbox"/>
Unannounced	<input type="checkbox"/>
Justification	
By	
Distribution/	
Availability Codes	
Dist	AV 1A 100/00
A-1	Special

UNCLASSIFIED

INTRODUCTION

In order to test high speed integrated circuits, the test setup should ideally make noninterfering connections to the output pins of the device under test. Currently, high end automated microcircuit test equipment make these connections with a minimum of 30pF of capacitive loading. As a result, some high speed devices may fail to operate in the test environment. The objective of this effort was to investigate and test methods of providing a high speed, low loading interconnection between the device under test and the automated tester using electro-optic techniques. The goals for this interconnection were; a greater than 1 GHz bandwidth, 50 mV sensitivity, real time acquisition, and scalability to more than 100 channels. The approach taken was to define a range of possible signal extraction methods and then search the available literature and do preliminary experiments to determine the best solution.

The range of techniques considered for signal extraction included direct and external modulation of semiconductor laser light. For laser based modulation both gain and loss control were considered. It was found that under gain controlled laser modulation using available semiconductor lasers, the maximum efficiency of the laser would cause unwanted current loading of the device under test. Using loss modulation in laser diodes, efficient modulation can be obtained with only small loading effects, however, these diodes are very temperature sensitive and will not give the necessary performance over a wide variety of temperatures. External modulation by electro-absorption was also inadequate due to temperature sensitivity. There are also polymers which exhibit electro-optic coefficients orders of magnitude greater than conventional crystals, but for some as yet unknown reason these effects fade with time. Another concept tested was the traveling wave modulator fabricated in GaAs or CdS, however they require polarizers and focussing elements which are too bulky to scale up to greater than 100 device pin test capability.

Finally, confined wave modulators were considered. The contractor purchased the equipment necessary to test this technique, and initial results seemed promising. The integrated Mach-Zender modulation can be directly connected to optical fibers without polarizers. From the data generated in preliminary experiments, this technique was the one determined to be the most viable in producing a low loading signal extraction method. However, more experimentation would be necessary to verify these initial findings. During the course of further study the Mach-Zender interferometer was accidentally destroyed beyond repair before definitive results could be obtained. Due to time and funding constraints it was not possible to purchase another Mach-Zender interferometer and remain within the scope of the effort.

Although the final goal of this effort (the fabrication of a working prototype) was not achieved, important groundwork in the search for a non-loading electro-optic signal extraction technique has been performed. Further study, perhaps in conjunction with some of the major automated microcircuit tester manufacturers, is necessary in order to see that the viable concepts explored in this effort become actual hardware which would revolutionize the test industry.

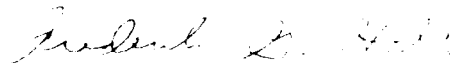

FREDERICK G. HALL
Reliability Physics Branch

TABLE OF CONTENTS

	PAGE
LIST OF FIGURES.....	3
LIST OF TABLES.....	4
INTRODUCTION.....	5
OPTICAL SIGNAL EXTRACTION TECHNIQUES.....	5
OPTICAL SOURCES AND MODULATORS.....	10
EXTERNAL OPTICAL MODULATION	12
REFERENCES	22

LIST OF FIGURES

Fig. 1	Signal extraction system schematic.....	5
Fig. 2	Optical power level versus modulation depth	10
Fig. 3	Typical laser diode characteristics	10
Fig. 4	Laser diode bias circuit	12
Fig. 5	Standard Mach-Zehnder waveguide modulator with coplanar waveguide electrodes.....	15
Fig. 6	Transmittance as a function of phase thickness for three values of reflectance.....	17
Fig. 7	Schematic for using the Fabry-Perot to test signals in IC pins.....	18
Fig. 8	Quantum confined excitons and their absorption spectrum.....	19

LIST OF TABLES

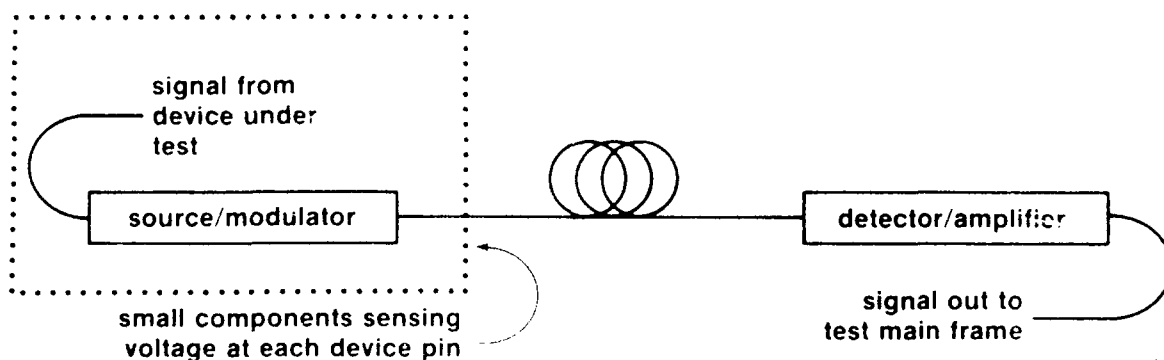
Table 1	Optical Power Level versus Modulation Depth	9
---------	---	---

INTRODUCTION

VLSI Technology has reached the point where single chips may require more than 100 external connections. These chips may also operate with clock rates of more than 50 MHz. The challenge to test such devices is not being met by complex automatic test equipment. Devices are driven by automatic testers which provide clocks and data at high speed as well as DC biases. Signals from the device under test (DUT) are then analyzed for possible errors. One of the factors limiting these multimillion dollar test machines is based on the fact that they use a 50 to 100 Ω cable to connect the output of the DUT to comparators for testing. In this arrangement, the combination of the cable impedance with the capacitance of the comparator circuit may induce failure in the DUT by drawing too much current. It was, therefore, necessary to develop some method of signal extraction that would not alter the test conditions. With this in mind, an investigation of optical signal extraction techniques was undertaken.

OPTICAL SIGNAL EXTRACTION TECHNIQUES

The following diagram shows schematically the form of an optical signal extraction system.



Z593

Fig. 1 Signal extraction system schematic.

With these building blocks, a system of equations may be written which defines the requirements on the source modulator system in terms of the overall system's bandwidth, sensitivity, and signal-to-noise ratio.

We begin with the following definitions:

- P_o = average optical power
- α = modulation ration
- K = optical loss ratio
- R = detector responsivity
- R_{in} = amplifier input impedance
- k = 1.38×10^{-23} J/°K Boltzman's constant
- T = temperature
- e = electronic charge
- B = bandwidth
- G = gain
- χ = added noise factor

Sources of noise

shot noise

$$i_{shot} = \sqrt{2eP_oRB}$$

Johnson noise

$$i_{johnson} = \sqrt{\frac{4kTB}{R_{in}}}$$

Added noise gain factor

$$i = G^1 + \chi (i_{noise})$$

↑

$$(i_{shot} + i_{johnson})$$

Now the total signal current is given by

$$S = \alpha P_o K R G \quad (1)$$

and the total noise current is

$$N = G(1 + \chi) (\sqrt{2eP_oRB} + \sqrt{4kTB R_{in}})$$

so

$$S/N = \frac{\alpha P_o K R}{G^{\chi} (\sqrt{2eP_oRB} + \sqrt{4kTB R_{in}})} \quad (2)$$

but, from (1)

$$G = \frac{S}{\alpha P_o K R}$$

Substituting this into (2) and solving for the modulation depth, we get

$$\alpha = \frac{1 + \chi \sqrt{S/N (\sqrt{2eP_oRB} + \sqrt{4kTB R_{in}})}}{P_o K R}$$

For application to signal extraction several of the variables in the above equation are defined.

$$k = 1.38 \times 10^{-23} \text{ J/}^{\circ}\text{K}$$

$$e = 1.6 \times 10^{-19} \text{ C}$$

$$T = 300^{\circ}\text{K}$$

$$B = 1 \text{ GHz or } 10^9 \text{ S}^{-1}$$

$$R = 0.7 \text{ for solid-state detectors or } 0.01-0.1 \text{ for photomultipliers } (\lambda > 650 \text{ nm})$$

$$R_{in} = 50 \Omega$$

$$S = 20 \text{ mA (This corresponds to 1 V into } 50 \Omega)$$

$$\chi = 0.2 \text{ for electronic amplifiers}$$

$$= 0.3 \text{ for avalanche photodiode amplification}$$

$$K = 1 \text{ for simplicity}$$

$$S/N = 30$$

These figures assume operation at room temperature; a bandwidth necessary to transmit >100 MHz square waves; 50 Ω operating environment; 1 V signal levels with 50 Ω final output; no optical losses; and a signal to noise ratio sufficient to see 30 mV signals.

Given these parameters, the modulation depth required of the modulator in response to a 1 V applied voltage is determined as a function of the optical power to be modulated and the type of detector. For photomultipliers, knowledge of the modulated wavelength is critical because photocathode characteristics vary widely, decreasing significantly with wavelengths longer than 633 nm. Further discussion will therefore center on PIN (P-layer, diode, structure; P-type, insulator, N-type) photodiodes and avalanche photodiodes (PPDs and APDs).

Avalanche photodiodes are solid-state detectors which generate internal gain due to cascading electrons under highly reverse biased conditions. They are generally capable of producing a maximum output current of 1 mA. They exhibit gain of around 100 and responsivity of about 0.7 A/W. These characteristics make them very useful for low light level applications. In this application, these detectors would require external amplification by a factor of 20.

The effects of external amplification are more evident when a PIN photodiode is used. While electronic amplification is not typically described in the same terms as the avalanche amplification inherent in APDs, an approximation based on the characteristics of a transistor based amplifier at 20 to 40 dB gains will be used. At 30 dB of gain, the added noise of an electronic amplifier is given by setting X at a value of 0.2 in the added noise equation. If n identical amplifiers were cascaded, the noise would grow as e^n . This coarsely justifies the use of the added noise equation.

It is apparent that the added noise for an external amplifier can be less than that of an avalanche amplifier. So in the end, a PIN photodiode proves to be the best choice as a detector. There are some devices currently on the market which attempt to integrate

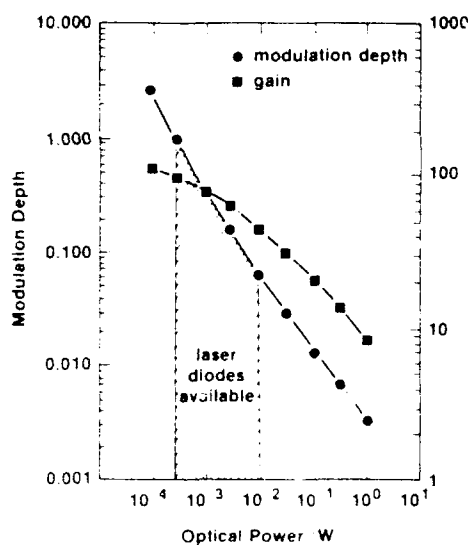
detectors with electronic amplifiers. Those which are designed for analog applications have no greater than a 1 GHz gain bandwidth product. This is not sufficient to realize the needed 20 to 40 dB of gain at 1 GHz. Other amplified photodiodes have high gain and frequency response, but they are integrated into optical communication receivers and produce digital output.

Now that the parameters of the detector/amplifier system have been stated, a function indicating the modulation depth required for a gain optical power level may be plotted.

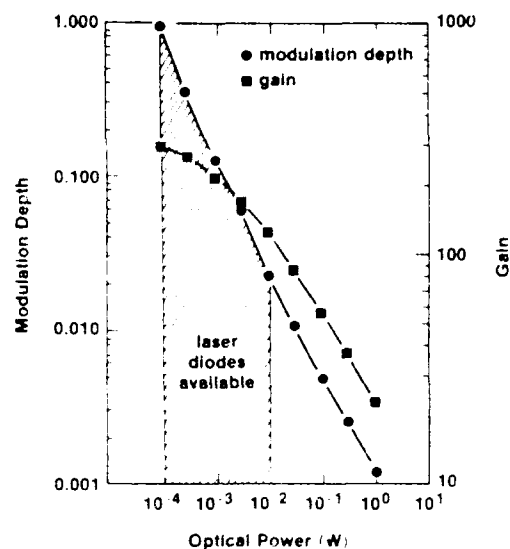
Table 1: Optical Power Level versus Modulation Depth

With Amplifier Noise				Without Amplifier Noise		
P	α	G	G(dB)	α	G	G(dB)
0.0001	2.64	108	41	0.969	295	49
0.0003	0.99	96.1	40	0.36	262	48
0.0005	0.639	89	40	0.36	216	47
0.001	0.359	79	39	0.13	216	47
0.003	0.152	63	36	0.06	170	45
0.01	0.0634	45	33	0.023	123	42
0.03	0.0301	32	30	0.011	86	36
0.1	0.0139	21	26	0.5%	56	35
0.3	.00703	13.5	23	0.26%	37	31
0.1	0.00340	8.4	18	0.125%	22.9	27

This provides a graphic illustration of the required modulation depth as a function of optical power. If we are limited by our choice of source or modulation to low optical power, we must provide both high modulation efficiency and high gain.



Z595

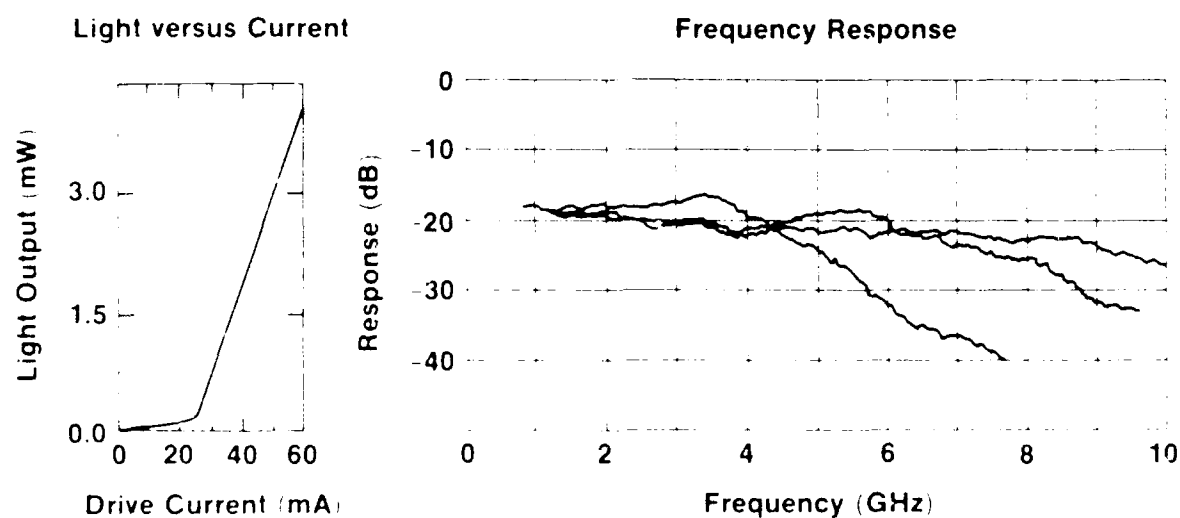


Z594

Fig. 2 Optical power level versus modulation depth.

OPTICAL SOURCES AND MODULATORS

The simplest approach to modulating light in a system involving fiber optics is to directly modulate a laser diode source. In this modulation scheme the number of carriers available in the semiconductor laser cavity is determined by the forward diode current.



Z596

Fig. 3 Typical laser diode characteristics.

From the light versus current plot, we can determine that the slope efficiency of the laser is 0.12 W/A and that this efficiency is achieved at optical power levels above 150 to 200 μ W.

η = slope efficiency of laser diode (W/A)

P_{\min} = minimum power at slope efficiency level

I_{\min} = minimum current at slope efficiency level

I_s = signal current

$$\alpha = \frac{P_s}{P_o} \leq \frac{\eta I_s}{P_{\min} + \eta I_s/2}$$

or assuming the limit of the inequality

$$I_s = \frac{\alpha P_{\min}}{\eta (1 - \alpha/2)}$$

For the diode given above, we have

$$P_{\min} = 0.2 \text{ mW}$$

$$\eta = 0.12 \text{ W/A}$$

$$0.1 < P_o < 3 \text{ (mW)}$$

At $S/N = 30$, the modulation depth ranges over

$$0.06 < \alpha < 1$$

and

$$0.1 < I_s < 3.3 \text{ (mA)}$$

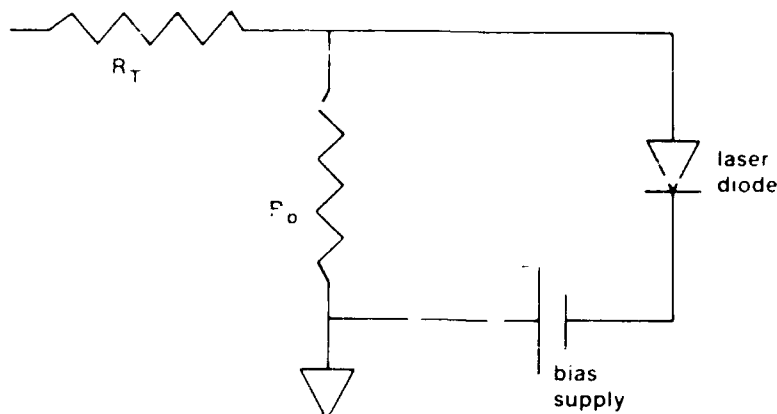
If a way can be found to supply the necessary bias current to the laser diode while allowing the DUT signal to supply modulating current an impedance of

$$Z = \frac{V_{\text{out}}}{I_s}$$

could be achieved, e.g., for $V = 1$ Volt

$$300 < Z < 10,000 \text{ (}\Omega\text{)}$$

A possible method for current bias:



Z597

Fig. 4 Laser diode bias circuit.

In this scheme, a resistor R_T isolates the DUT from the laser diode and its bias. The signal current passing this resistor is divided between the diode and R_o . The bias current is also passed by R_o . The noise current due to thermal fluctuations in R_T which passes through the laser diode is $0.25 \mu A$; far below the mA level required for bias. This means that the bias network adds no significant noise.

Further consideration must include dissipation of heat by the resistor network as well as by the laser diode. In a rough approximation, the majority of heat is generated by the signal in the terminating resistor and by the bias current in the laser diode. These calculate as follows:

$$P_{RT} \leq I_S^2 R_T \approx 10 \text{ mW/channel}$$

$$P_{Laser} \leq I_{Bias}^2 R_{Laser} \approx 7.5 \text{ mW/channel}$$

At $<20 \text{ mW/channel}$, 100 channels would have $<2 \text{ W}$ of power to dissipate.

EXTERNAL OPTICAL MODULATION

Another approach to optical signal extraction is to use a continuous wave (cw) laser diode with an external modulator. There are several ways in which light may be modulated. They all involve changing some property of the light such as polarization,

phase, frequency, or amplitude. At the detector end of the system, it is only capable of sensing a change in amplitude. Therefore, whatever type of modulation is accomplished at the DUT must be converted to amplitude modulation before the detector.

Frequency modulation, if it is not accomplished by affecting the optical source, is only possible with high power levels or extremely long interaction lengths. These are not possible under the constraints of this application. Each of the remaining modulation types has a form in which conversion to amplitude modulation is possible. Phase modulation is converted to amplitude modulation by interference. An interferometer is a device which compares a phase shifted beam of light with a reference beam. The coherent sum of two beams having a phase difference of δ is given by:

$$I = 4I_1 \cos^2 \delta/2$$

where δ is the phase difference between two beams of light having equal intensity and frequency. It is by a similar effect that polarization modulation is converted to amplitude modulation.

In this case, two orthogonal components of a beam provide the phase shifted and reference beams and a polarizer sums components of the two beams to yield intensity modulation. In both phase and polarization modulation, the change in phase may be produced on a fast time scale by altering the indexes of refraction of the material by the application of an electric field. The change in index Δn corresponds to the change in phase δ through material and design parameters.

$$\delta = \frac{2\pi\Delta nL}{\lambda_0} = \frac{\pi n^3 r_c EL}{\lambda_0},$$

where L is the light-field interaction length, λ_0 is the wavelength of the light in vacuo, n is the materials index of refraction at λ_0 , E is the electric field strength in the interaction region, and r_c is the material's electro-optic coefficient.

Since 100% modulation occurs with a phase change of π , a modulation depth may be approximated as a function of applied voltage, V_s , and the geometry dependent voltage necessary to achieve a phase delay of π radius, V_π :

$$\alpha = \frac{\pi}{2} \frac{V_s}{V_\pi}$$

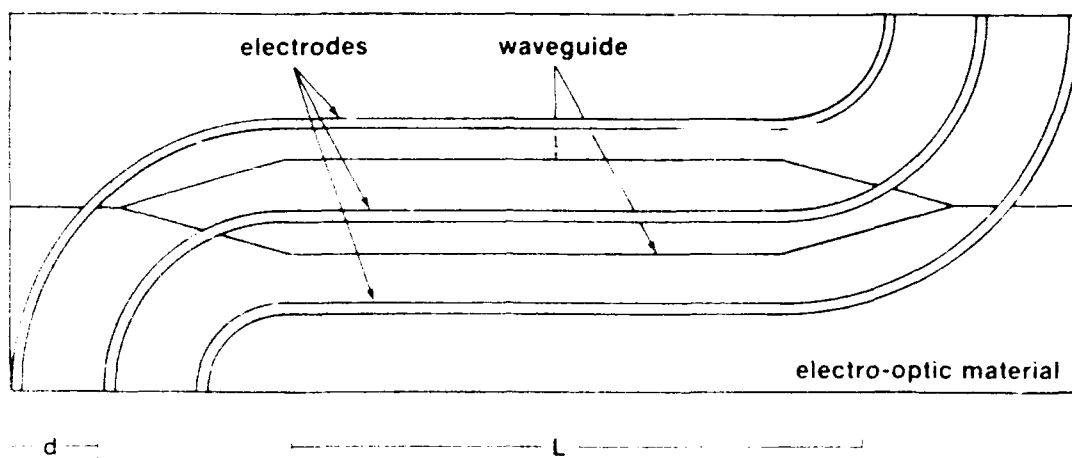
For efficient phase or polarization modulation, it is advantageous to make a long modulator with narrow electrode spacing. This allows a high electric field and long interaction distance with moderate applied voltage. This can be demonstrated in the equation for V_π if the electric field is approximated to be that occurring between two plates of a parallel plate capacitor of separation d and length L .

$$V_\pi = \frac{\lambda_o}{n^3 r} \frac{d}{L}$$

so

$$\alpha = \left(\frac{\pi n^3 r L}{2 d \lambda_o} \right) V_s$$

To be more specific about the form of a phase modulator, and in particular one with a low V_π , integrated optics may be employed to increase the electro-optical interaction length. A common type of integrated optical modulator is the guided wave Mach-Zehnder interferometer. This modulator uses a symmetric waveguide structure to split a single guided wave into two such waves; modulate the phase of one relative to the other; and to recombine the two interferometrically to achieve intensity modulation. A typical modulator is illustrated below.



Z598

Fig. 5 Standard Mach-Zehnder waveguide modulator with coplanar waveguide electrodes.

Dimensions for such modulators may be

$$d = 8 \mu\text{m}$$

$$l = 4 \text{ mm}$$

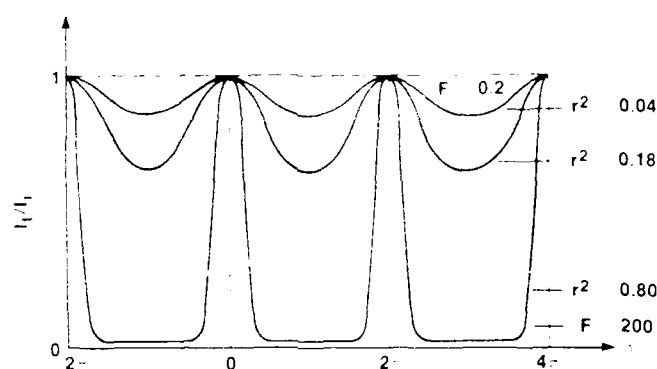
A modulator of this type may also have a 33 ps response time corresponding to 10 GHz. Commercial vendors produce these modulators with similar specifications. This design has a capacitance of about 3 pf which corresponds to about 50Ω at 1 GHz. This method of modulation has gained a high degree of acceptance in the fiber optics community over those methods employing polarization modulation because it does not require polarizers. For this reason and because there are no other advantages, polarization modulation was not pursued further.

There is another style of modulators used extensively by researchers in optical communications. That is the directional coupler. It has the advantage that a cross-point switch array can be produced which allows signals from any of n input ports to be independently rerouted to any of n output ports. The switch works by electro-optically controlling the evanescent coupling length of two waveguides. In this application there is no need for cross-point switching and the directional coupler has a particular disadvantage

which is minimized in the Mach-Zehnder structure. The problem is that the directional coupler depends on achieving an absolute path length for waveguide interaction. This path length is dependent on material, temperature, and stress. In the Mach-Zehnder, however, the interference depends on a relative change in optical path length between two paths which are located in very close proximity to each other. In that case stress and temperature are not likely to cause a large relative phase shift. No specific data on the temperature dependence of phase shift in electro-optic materials was found in the literature so a quantitative argument is not possible here. A final consideration for the guided wave modulator is the optical power capability. Two factors come into play here. The first is a materials problem. At wavelengths below $1.3\text{ }\mu\text{m}$ the effects of photorefractive damage in the waveguides may cause failure. Photorefractive damage is a change in index due to the migration of charges in the waveguide region. This occurs as impurities in a LiNbO_3 waveguide are ionized by light. As charges separate, their electric fields induce index changes in the material. The local changes in index scatter light out of the waveguides making the whole system lossy. Since these index changes arise through the same mechanism that provides modulation in the first place, more efficient electro-optic materials are typically more sensitive to photorefractive damage. New processes for Ti:LiNbO_3 crystals and for diffusing waveguides have raised the damage threshold to about 10 mW for 830 nm . The second factor regarding the optical power capability of these structures is the fact that they are single mode devices. This means that efficient optical coupling is difficult to achieve. Typically the single mode input will show as much as a 10 dB power loss (i.e., a factor of 3). The same loss also applies to the source laser. The availability of $>10\text{ mW}$ laser diodes requires that a system having 20 dB losses at a signal to noise ratio of 30 have 20% modulation depth. Such systems are advertised by more than one company.

In looking at nonguided-wave modulators, there are ways to improve modulation depth by making multiple passes through an electro-optic medium with a free-propagating beam. As with guided waves, the goal is to enhance the modulator sensitivity by

increasing the ratio between electro-optic interaction length and electrode separation. One optical device which allows a long interaction length in a relatively small package is the Fabry-Perot interferometer. This instrument is made by placing two partially reflecting mirrors parallel to each other. Successive reflections of a beam passing through the mirror set interfere with each other yielding output phase and intensity as a function of the mirror to mirror round trip time, the optical frequency, and the mirror reflectivities and losses.



Z601

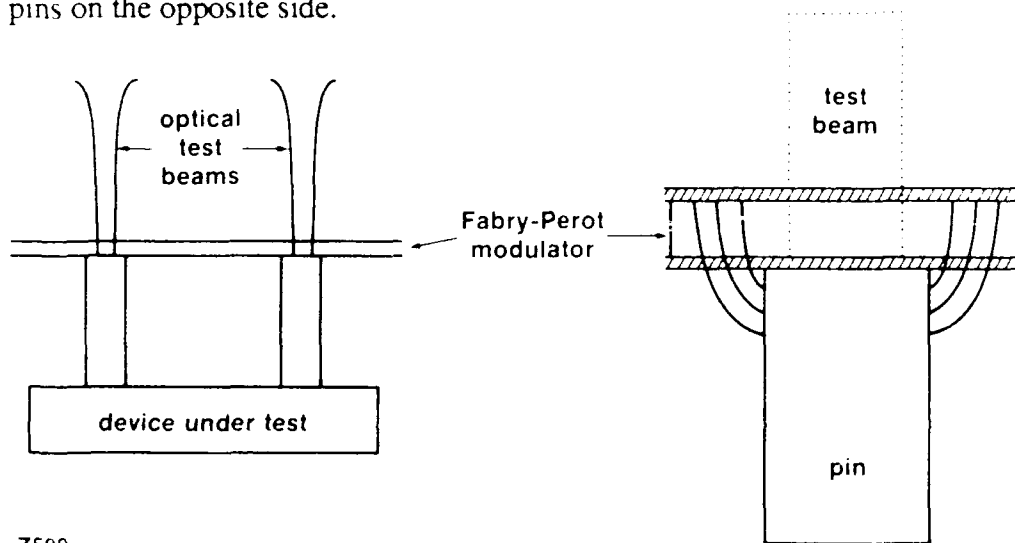
Fig. 6 Transmittance as a function of phase thickness for three values of reflectance.

This optical cavity acts best as an amplitude modulator when the mirrors are lossless and have equal reflectivities. In that case, the transmitted portion of a narrow monochromatic band beam follows the form of an airy function where δ is the optical phase delay associated with one round trip in the Fabry-Perot. The finesse, $F \equiv \frac{\pi\sqrt{R}}{2}$, is the ratio between the peaks of the airy pattern and the full width at half max of the peaks, and $F \equiv \left(\frac{2\sqrt{R}}{1-R^2}\right)^2$ for equal reflectivities of R .

This interferometer can be made into an electro-optical device by filling the space between the mirror with an electro-optic material. This allows the phase shift δ in the Fabry-Perot cavity to be electric field dependent. The sensitivity of this type of modulator

is greater than that of a modulator without mirrors by a factor of finesse. At the same time, the response time of the modulator is increased by the same factor.

In actual use, one could envision a Fabry-Perot interferometer with a finesse of 100 and a spacing of slightly $< \lambda/2$. This design would allow for 50% transmission with no applied field in order to achieve maximum sensitivity (dI/dE change in intensity with respect to electric field strength). A transparent conductive coating placed on one side of the modulator could act as a reference plane drawing electric field lines from the test devices output pins on the opposite side.



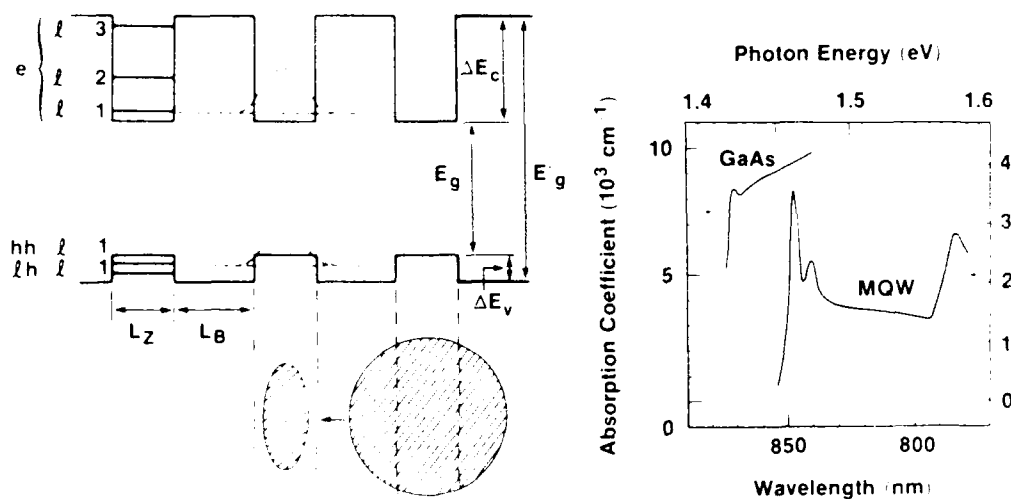
Z599

Fig. 7 Schematic for using the Fabry-Perot to test signals in IC pins

With this type of modulator there are a few practical limitations. Because the transmission function is such a strong function of wavelength, it is necessary to have a source laser with a bandwidth less than half the full width at half max of the transmission peak in frequency space (i.e., $\Delta\nu < c/4n\ell F$). The temperature variation of the device must also be minimized to prevent a change in the peak location by as much as the same amount. Finally, losses must be minimized as they effect the finesse of the cavity. By using a first order Fabry-Perot where the spacing is $\sim \lambda/2$, these problems may be minimized. The problem then becomes one of finding an electro-optic material which may be grown or deposited to

a thickness of $<1\ \mu\text{m}$. Work is currently under way to develop both single crystal and organic thin films. So far, a Fabry-Perot has not been demonstrated with characteristics appropriate to signal extraction.

While developments have been occurring in optical devices, there has also been a considerable effort in the development on new optical materials. One of the goals in this area of work has been to engineer a material which would exhibit large changes in refractive index or in absorption with applied electric fields. The product of lattice engineering is multiquantum-well material. In a multiquantum-well structure (MQWS) a crystalline structure is grown which alternates between a high bandgap material to a low bandgap material. The thickness of these layers can be controlled in growth to a single atomic monolayer. Such materials have useful effects for application to modulators when the thickness of the low bandgap material is comparable to the electron-hole correlation distance. This allows correlated electron-hole pairs (or excitons) to be formed which are observable at room temperature.



Z600

Fig. 8 Quantum confined excitons and their absorption spectrum.

In the absorption spectra shown above, a residual excitonic absorption peak may be seen in the bulk GaAs absorption. In the MQWS absorption, there are two peaks in absorption, one due to the formation of light hole excitons and the other due to heavy hole exciton formation. Once excitons are formed by photo ionization of electron holes, they have very short lifetimes on the order of only 0.4 ps.

Now let us consider the effects of electric field on excitonic absorption. There are two cases to be considered here. First, there is the case where an electric field is applied parallel to the quantum well planes. In this case, a deformation of the atomic potential wells occurs, resulting in a polarization of the excitonic static resulting in a lower energy state. Hence the band edge shifts to the very slightly red end of the spectrum. Before much shift in energy can occur, the electric field ionizes the excitons resulting in a shorter lifetime and a broadening of the excitonic resonances. In the other case, an electric field is applied normal to the plane of the quantum wells. The potential wells are deformed causing a shift in the carrier distribution and a substantial drop in the energy of system. Field ionization can also occur, resulting in line broadening.

Of these effects, the quantum confined stark shift with an electric field applied normal to the plane of the quantum wells is the most interesting for our application. It is possible to use this effect to see a change in optical index, but more direct amplitude modulation can be obtained by using the absorption edge.

The possibility of using these materials for signal extraction is exciting because of their incredible sensitivity. Samples having submicron thickness may change their absorption by as much as a factor of 10 with a voltage applied of only 1 V. There are several limitations to the use of quantum wells, however. the effect of external electric fields on excitonic states is so dramatic that the excitons only exist over a dynamic range of about 10. Thus, it would be possible to use MQWS as threshold detectors, but not as voltage encoders. The other problem encountered with MQWS is the limitation on photon flux. At a power density of about 500 W/cm² the excitonic states are saturated. An

argument based on the Pauli exclusion principle works well to describe experimental saturation results. The latter problem is critical at very high speeds when modulator dimensions on the order of microns are necessary. The limitation is then improved by capacitance restraints. If we wish to apply 5×10^4 V/cm with 1 V, a separation of $0.2 \mu\text{m}$ is required. A capacitance of 1 pf gives an area of $2 \times 10^{-5} \text{ cm}^2$; saturation then occurs at 10 mW of optical power. The final consideration for MQWS is that they must be temperature controlled to prevent line shift. This is equivalent to the shift seen in bulk GaAs where the energy gap is given empirically by

$$\epsilon(T) = 1.519 - 5.405 \times 10^{-4} T^2 / (T + 204) \quad (\text{eV})$$

At 300°K , we have a shift of $4.5 \text{ meV}/^\circ\text{K} = 0.03\%/^\circ\text{K}$, $\sim 2.6 \text{ \AA}/^\circ\text{K}$ at 850 nm . Whereas the exciton peak shift at 300°K and $5 \times 10^4 \text{ V/cm}$ a shift of 25 meV/V or 14 \AA/V (across $0.2 \mu\text{m}$) occurs at 850 nm . Thus, for $\pm 30 \text{ mV}$ stability, $\pm 0.17^\circ\text{K}$ temperature stability is required.

Another area of development in electro-optic materials is polymer science. By various techniques, materials are deposited on ordinary substrates which show electro-optic effects. To date, a concerted study of these materials has been suppressed due to proprietary interests. Several groups have shown electro-optic effects larger than those observed in LiNbO_3 (a favorite material for electro-optics in the visible). Most of the published results on these materials concentrated on harmonic conversion. While these results have some connections to operation of organic polymers in electronic and opto-electronic applications, this effort did not allow sufficient opportunity to investigate their relations in order to make a reasonable comparison. Also, these materials are lacking in terms of optical quality and reproducibility.

REFERENCES

1. K. D. Singer, S. J. Lalama, and J. E. Sohn, "Organic Nonlinear Optical Materials," Integrated Optical Circuit Engineering II, S. Sriram, editor, Proc. SPIE 578 (1985) p. 130.
2. S. J. Lalama, J. E. Sohn, and K. D. Singer, "Organic Materials for Integrated Optics," Integrated Optical Circuit Engineering II, S. Sriram, editor, Proc. SPIE 578 (1985) p. 168.
3. T. E. Van Eck, P. Chu, W. S. C. Chang, and H. H. Wieder, "Electroabsorption in an InGaAs strained-layer multiple quantum well structure," Appl. Phys. Lett. 49, 135 (1986).
4. W. H. Knox, R. L. Fork, M. C. Downer, D. A. B. Miller, D. S. Chemla, and C. V. Shank, "Femtosecond Dynamics of Resonantly Excited Excitons in Room-Temperature GaAs Quantum Wells," Phys. Rev. Lett. 54, 1306 (1985).
5. D. S. Chemla, D. A. Miller, and P. W. Smith, "Nonlinear Optical Properties of Multiple Quantum Well Structures for Optical Signal Processing," in Semiconductors and Semimetals, Chap. 5, Edited by R. Dingle, R. W. Willardson, and A. C. Beer, (Academic Press, Inc., New York, 1987).
6. G. Hernandez, Fabry-Perot Interferometers (University Press, Cambridge, 1986).



MISSION of *Rome Air Development Center*

RADC plans and executes research, development, test and selected acquisition programs in support of Command, Control, Communications and Intelligence (C³I) activities. Technical and engineering support within areas of competence is provided to ESD Program Offices (POs) and other ESD elements to perform effective acquisition of C³I systems. The areas of technical competence include communications, command and control, battle management information processing, surveillance sensors, intelligence data collection and handling, solid state sciences, electromagnetics, and propagation, and electronic reliability/maintainability and compatibility.